Giant Magnetostrictive Material-Fiber Bragg Grating Magnetic Field Sensors used in Magnetic Bearings

Jiayi Liu[a], Guoping Ding[*b], Bin Gao[b], Biyun Zhang[b]

[a]School of Information Engineering, Wuhan University of Technology, Luoshi Road, 430070 Wuhan, Hubei, China
[b]School of Electromechanical Engineering, Wuhan University of Technology, Luoshi Road, 430070 Wuhan, Hubei, China
dgp7910@163.com

***Abstract*—A novel FBG-GMM sensor was proposed to measure magnetic flux density, in which the FBG was stuck perpendicular to the GMM's principal magnetostriction orientation to make a thin-slice sensor. The FBG-GMM magnetic field sensor's properties were tested on a U-shape electromagnet test setup, the measured data were consistent with the theoretical prediction and the sensor' linear range is from 0.2T to 0.6T. The FBG-GMM magnetic field sensor was introduced to measure a radial magnetic bearing's air-gap flux density. Static flux density measurement was performed through two FBG-GMM sensors and one temperature compensation FBG, and the measured data were consistent with the sensor properties obtained from the U-shape electromagnet test, which validate the FBG-GMM magnetic field sensor's feasibility.**

I. INTRODUCTION

A magnetic bearing utilizes magnetic forces to levitate a rotating shaft in the bearing stator that includes actuator control coils, and a narrow air-gap separates the bearing stator and the rotor. In analyzing the behavior and performance of a magnetic bearing, the primary objective is to determine the forces generated by the actuator in response to currents of the coils and motion of the rotor. The magnetic field is physical medium of magnetic levitation and motion control, which essentially describes the coil/geometry–forces relationship. Due to the essential open-loop instability of the magnetic bearings system, the magnetic field is of remarkable dynamic and nonlinear features.

Normally magnetic circuit or finite element methods are used to predict magnetic field in magnetic bearings. However these theoretical analyses have inevitable limitations that their assumptions, models or boundary conditions cannot accurately describe magnetic field features, especially when the magnetic bearings operate at nonlinear region. So it is necessary to perform magnetic field online measurement to accumulate data for future design calculations and even online control.

This paper proposed a fiber Bragg grating (FBG) based Giant Magnetostrictive Material magnetic field sensors for magnetic bearings. Fiber Bragg grating sensors offer several significant advantages over conventional electrical sensors, such as immunity to electromagnetic noise and radio frequency interference, easy multiplexibility, small size, light weight, corrosion resistance and higher temperature capability. FBG sensors have become an important class of sensing device for long-distance and distributed sensing of various types of physical parameters such as strain, pressure, temperature, etc. in a broad domain of industrial fields. However, FBG sensors fall short of any magnetic field sensing because of their inherently weak magneto-optical Faraday effect. Recently, it has been demonstrated that a FBG can be stuck onto a Giant Magnetostrictive Material(GMM) to form a GMM–FBG sensor for magnetic field or electric current sensing[1-5]. *TbDyFe*, whose saturation magnetostriction is approximate 2000ppm, is one of the most promising giant magnetostrictive materials. It will expand when being put in magnetic field, which has a linear and reverse response to the strength of the magnetic field. If these magnetostrictive materials are bonded with an FBG fiber, the elongation of the magnetostrictive film due to magnetic field will result in a change in grating period in FBG fiber, and therefore generate a shift of the FBG central wavelength. In this way the drift of the FBG wavelength to the magnetic field response is correlated. Compared to conventional non-optical magnetic field or electric current sensors such as Hall-effect sensors and reluctance coils, this type of GMM–FBG sensor features a high level of immunity to electromagnetic interference, a great potential for large-scale multiplexing and a large capability for self-reference.

This paper proposed a novel FBG-GMM sensor to measure magnetic flux density, in which the FBG was stuck perpendicular to the GMM's principal magnetostriction orientation to make a thin-slice sensor to be used in magnetic bearings. Firstly, a U-shape electromagnet test setup was constructed and the GMM–FBG magnetic field sensor's static properties were tested. Then the GMM–FBG magnetic field sensor was introduced to magnetic bearing's air-gap flux density measurement. A radial magnetic bearing test setup was constructed and the air-gap flux density was measured through two FBG-GMM sensors and one temperature compensation FBG in static conditions

II. FBG-GMM MAGNETIC FIELD SENSOR

A. Giant Magnetostrictive Material (GMM)

A magnetostrictive material develops large mechanical deformations when subjected to an external magnetic field as shown in Fig.1. This phenomenon is attributed to the rotations of small magnetic domains in the material, which are randomly oriented when the material is not exposed to a magnetic field. The orientation of these small domains by the imposition of the magnetic field creates a strain field. As the intensity of the magnetic field is increased, more and more

* Corresponding author: dgp7910@163.com; Tel:0086-18071110860; Fax:0086-27-87651793

magnetic domains orientate themselves so that their principal axes of anisotropy are collinear with the magnetic field in each region and finally saturation is achieved.

An equation about Giant Magnetostrictive Material should be taken into consideration:

$$\delta = \varepsilon_{GMM} = \frac{\Delta l}{l} \tag{1}$$

In this equation, δ is the magnetostrictive coefficient, ε_{GMM}, l and Δl is the strain, original length and elongation of the magnetostrictive material respectively.

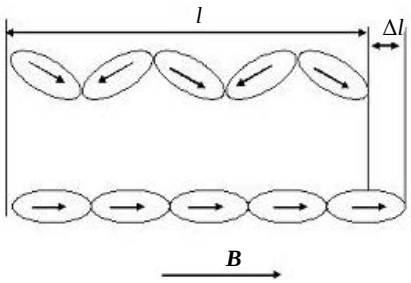

Fig.1 Magnetostriction

Some magnetostrictive material, such as *RFe*, *TbDy* and *TbDyFe*, has much lager magnetostrictive coefficient, higher energy density and response speed than normal ones and is called Giant Magnetostrictive Material (GMM).GMM is widely used in many research fields such as the measurement of magnetic field, sonar system, shock mitigation system. In this paper, we used *TbDyFe* as sensitive material whose magnetostriction curve is shown in Fig. 2.

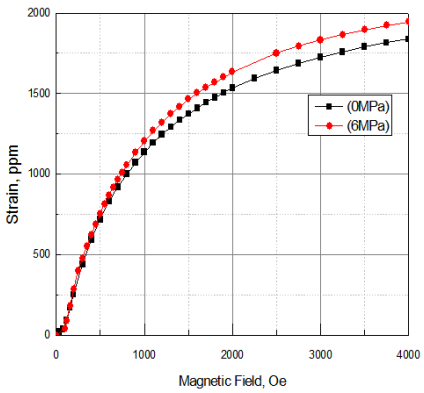

Fig.2 Magnetostriction curve of *TbDyFe*

B. Sensing Principle of Fiber Bragg Grating(FBG)

The fiber Bragg grating (FBG) is photo-inscribed into an optical fibre using a high power UV laser beam and is associated with a small periodic refractive index variation in the fibre core. Fig. 3 shows the basic sensing principle of an FBG. When the light of a broadband spectrum is guided through the optical fibre to the FBG, a narrow band component as indicated by the spike in the reflection spectrum is reflected back at the Bragg resonance wavelength, given by:

$$\lambda_B = 2n\Lambda \tag{2}$$

Where Λ is the grating pitch and n is the fibre refractive index of the core. In Eq. (2) it can be seen that the Bragg wavelength is changed with a change in the grating pitch or the effective refractive index.

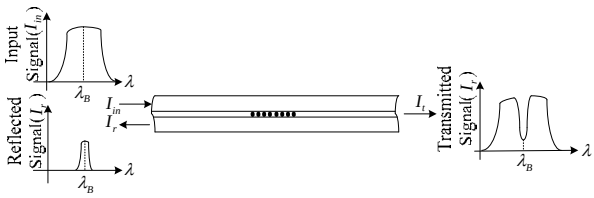

Fig. 3 Sensing principle of FBG

The Bragg wavelength is strain-dependent and temperature-dependent. The strain response arises due to both the physical elongation of the sensor (and corresponding fractional change in grating pitch), and the change in fiber index due to photo-elastic effects, whereas the thermal response arises due to the inherent thermal expansion of the fiber material and the temperature dependence of the refractive index. The shift in Bragg wavelength with strain and temperature can be expressed using

$$\Delta\lambda_B = 2n\Lambda\left(\left\{1-\left(\frac{n^2}{2}\right)[P_{12}-\nu(P_{11}+P_{12})]\right\}\varepsilon+\left[\alpha+\frac{(\frac{dn}{dT})}{n}\right]\Delta T\right) \tag{3}$$

where ε is the applied strain, $P_{i,j}$ coefficients are the Pockel's (piezo) coefficients of the stress-optic tensor, ν is Poisson's ratio, and α is the coefficient of thermal expansion of the fiber material (e.g., silica), and ΔT is the temperature change. The factor $\left(\frac{n^2}{2}\right)[P_{12}-\nu(P_{11}+P_{12})]$ has a numerical value of ≈ 0.22. The measured strain response at constant temperature is

$$\frac{1}{\lambda_B}\frac{\delta\lambda_B}{\delta\varepsilon} = 0.78\times10^{-6}\,\mu\varepsilon^{-1} \tag{4}$$

This responsivity gives a "rule-of-thumb" measure of the grating shift with strain of 1 nm per 1000 $\mu\varepsilon$ at 1300nm. In silica fibers, the thermal response is dominated by the d*n*/dT effect, which accounts for 95% of the observed shift. The normalized thermal responsivity at constant strain is

$$\frac{1}{\lambda_B}\frac{\delta\lambda_B}{\delta_T} = 6.67\times10^{-6}{}^{\circ}C^{-1} \tag{5}$$

In this paper, we used FBGs of about 1300nm wavelength, that a wavelength resolution of 1 pm (0.001 nm) is required to resolve a temperature change of 0.1℃, or a strain change of 1 μ strain.

C. FBG-GMM Magnetic Field sensor

The FBG-GMM magnetic sensor's principle is that the FBG stuck onto the GMM detects the GMM's stain induced by magnetostriction when it is exposed to magnetic field. Normally the FBG was stuck onto the GMM along its principal magnetostriction orientation to constitute a FBG-GMM magnetic field sensor as shown in Fig.4 (a).

However this configuration was not feasible for magnetic bearing's air-gap flux density measurement. The main reason was that the magnetic bearing's air-gap was too narrow to accommodate the FBG as it was stuck along the flux density orientation, which was also the GMM's principal magnetostriction orientation.

Therefore, we customized a 1.5mm-thick *TbDyFe* slice whose principal magnetostriction is along thickness orientation. When the *TbDyFe* slice was stuck onto the magnet pole's end surface, the flux density passing through the *TbDyFe* slice produced magnetostriction along thickness orientation. Since the FBG's length (almost 10mm) is much larger than the air-gap's thickness, the FBG was stuck onto side of the *TbDyFe* slice along its length orientation, which is perpendicular to the principal magnetostriction orientation as shown in Fig.4 (b). Fortunately, *TbDyFe* is of quasi-linear magnetostriction that means magnetostriction along thickness orientation causes relevant deformation along length and width orientation, and volume of *TbDyFe* slice almost maintains the same. Therefore the above adaptation was feasible in principle and it was necessary to test this novel FBG-GMM sensor's properties before its practical application.

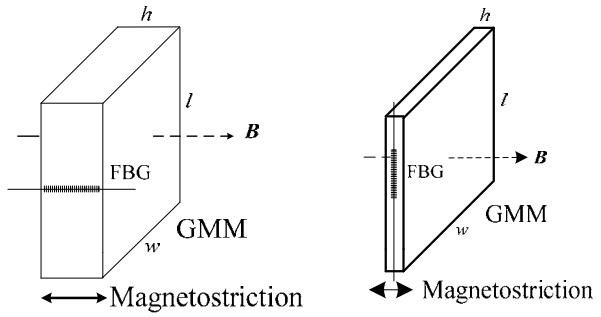

Fig.4 FBG-GMM magnetic field sensor
(a)FBG was stuck along principal magnetostriction orientation
(b)FBG was stuck perpendicular to the principal magnetostriction orientation

III. TEST OF FBG-GMM MAGNETIC FIELD SENSOR PROPERTIES

Based on the basic principle of the FBG-GMM magnetic sensor proposed in Section II, a set-up was constructed to test the FBG-GMM magnetic field sensor's properties including linearity, sensitivity, and range.

Fig.5 shows the schematic diagram of the test set-up, which was composed of a pair of U-shape electromagnets powered by two DC supplies, a FBG-GMM magnetic sensor and a FBG wavelength demodulator connected with a computer.

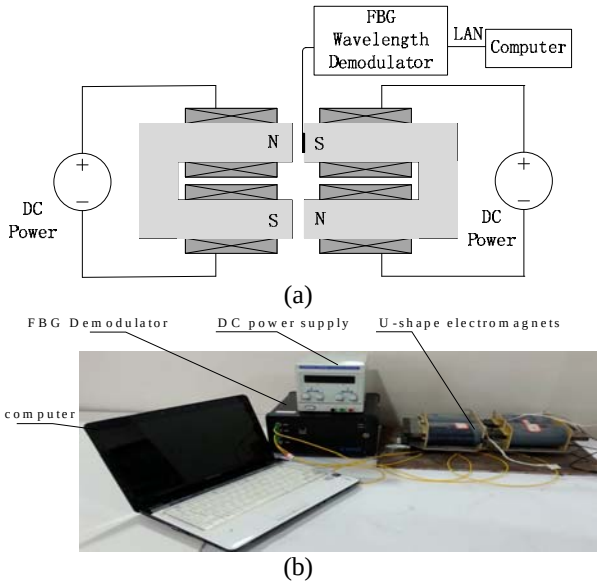

Fig.5 A test set-up of the FBG-GMM sensor's properties
(a) schematic diagram (b) actual system

Each U-shape electromagnet was made of a 30-piece silicon steel lamination stack wound with an 800-turn coil. The air-gap between the two electromagnets was fixed at 5mm, and a FBG-GMM magnetic sensor was stuck onto the surface of one electromagnet's pole to measure the flux density in the air-gap. FBG-GMM magnetic sensor's wavelength shift was demodulated and sent to the computer.

In the static properties test, DC currents from 0.1A to 2.2A with an interval of 0.1A were applied on the coils. A basic magnetic circuit equation shown in (6) was used to calculate the air-gap flux density according to the applied DC currents.

$$B_0 = \frac{\mu_0 N * I}{x_0} \tag{6}$$

where, $\boldsymbol{B}_0$ is the air-gap flux density, μ_0 is the magnetic permeability of a vacuum, N is number of the coils, I is the current applied on the coils and x_0 is the length of the air-gap.

It should be mentioned that since the air-gap between the electromagnet pair was large enough to dissipate the heat and the applied current was relatively small, we ignored the temperature effort on the sensor. Moreover, a Gauss-meter was also used to measurement the air-gap flux density to validate the calculated flux density

The FBG-GMM sensor's wavelength shift relevant with air gap flux density is illustrated in Fig.6

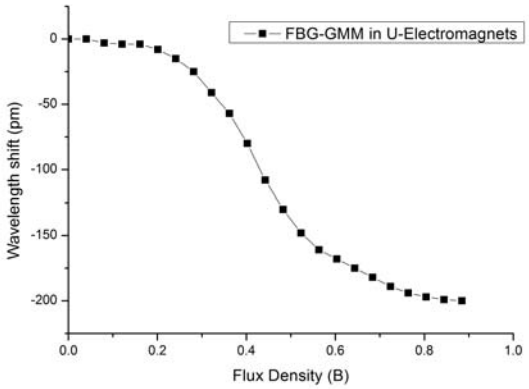

Fig.6 FBG-GMM sensor's wavelength shift relevant with air-gap flux density (DC currents, U-Electromagntes)

In Fig.6, the FBG's wavelength shift was negative with flux density from 0 to 0.9T, and it decreased with increasing flux density. It was consistent with the theoretical prediction that when the flux density increased, the GMM slice's thickness increased while its length and width decrease to remain the same volume. Shrink of the length caused decrease of FBG wavelength shift.

Moreover, the FBG-GMM sensor's wavelength shift curve could be divided to three parts. The first part, from 0 to 0.2T, it seemed like a "dead zone" where the wavelength shift varied very slightly; the second part, from 0.2T to 0.6T, the wavelength shift decreased almost linearly with increasing flux density; and the last part, from 0.6T to 0.9T, the wavelength shift curve slowed down to saturation. Although the total wavelength shift was about 200pm, amount to 200$u\varepsilon$ with a 1300um-center wavelength, which was almost a tenth of the strain produced by *TbDyFe* principal magnetostriction, it was large enough for the air-gap flux density measurement.

IV. FBG-GMM MAGNETIC FIELD SENSOR USED IN MAGNETIC BERINGS

Based on the tests of the FBG-GMM magnetic sensor's properties in Section III, the sensor was introduced to magnetic bearings for the air-gap flux density measurement. Fig. 7 depicts the sensors detail and their mounted positions in a radial magnetic bearing. Two FBG-GMM magnetic sensors were stuck onto the surface of a magnet pole (pole 7), especially, since the bearing's air-gap was too narrow to dissipate the heat and the FBG was sensitive to temperature variation, an additional FBG was stuck onto the surface of the same magnet pole to measure the temperature variation and to be used to compensate the temperature influence on the FBG-GMM magnetic sensors.

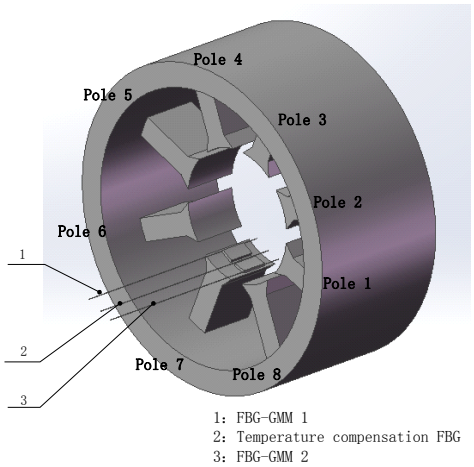

(a)

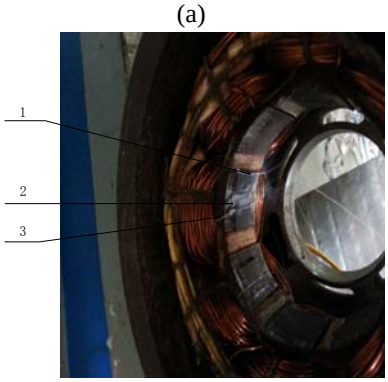

(b)

Fig.7 FBG-GMM sensors mounted in a radial magnetic bearing
(a) schematic diagram (b) actual device

Fig.8 shows the measurement system constructed to perform the magnetic bearing's air-gap flux density measurement. In the system, a motor with a frequency converter drove the rotor through a coupling, and a DC power supply provided currents to the coils wound on the magnet poles of the radial bearing, and the FBG-GMM magnetic sensor's wavelength shift was demodulated and sent to the computer.

The radial magnetic bearing was of an 8-pole structure with NNSS configuration. The rotor's inner diameter and outer diameter were respectively 45mm and 66mm. The stator's inner diameter and outer diameter were respectively 71mm and 144mm. The air-gap between the rotor and the stator of this radial bearing was fixed at 2.5mm. Each magnet pole-pair had a 334-turn coil.

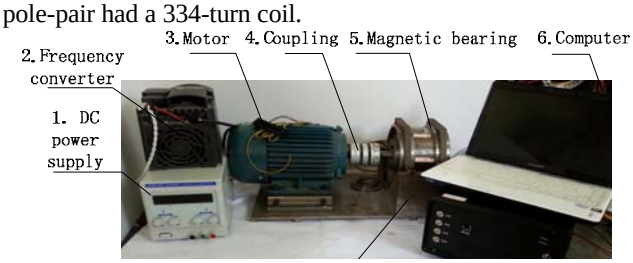

Fig.8 A test set-up of the FBG-GMM sensor's properties used in magnetic bearings
(a) schematic diagram (b) actual system

In this paper we focused on the feasibility and basic properties of the sensor, so the air-gap flux density was measured in static condition that was static rotor with DC currents excitation. DC currents from 0A to 4.8A with an interval of 0.2A were applied on the coils of one pole pair (pole 6 and pole 7). The air-gap flux density was calculated based on the magnetic circuit equation shown in (6).

Fig. 9 shows the wavelength shift of the two FBG-GMM sensors and the temperature compensation FBG.

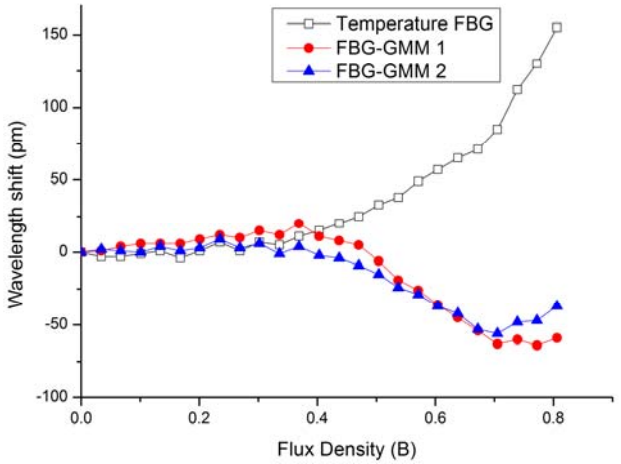

Fig.9 FBG-GMM sensor and temperature compensation FBG wavelength shift

In Fig. 9 the maximum wavelength shift of the temperature compensation FBG reached about 150pm, according to the temperature sensibility illustrated in Section II, the temperature increment was about 15℃ as the currents reached 4.8A, which meant the temperature effect on the FBG-GMM sensors could not be ignored.

The temperature FBG's wavelength shift was subtracted from the FBG-GMM sensors' wavelength shift to get the temperature compensation. Fig.10 shows the compensated wavelength shift of the two FBG-GMM sensors.

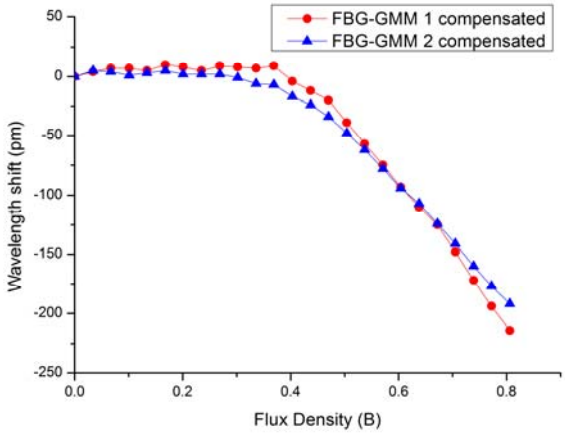

Fig.10 Compensated wavelength shift of the two FBG-GMM sensors

In Fig. 10 the compensated wavelength shift of the two FBG-GMM sensors had very similar tendency, which was also consistent with the wavelength shift curve obtained from U-electromagnets experiment shown in Fig.6. It can be concluded that the FBG-GMM sensor was feasible to be used to measure the air-gap flux density of magnetic bearings.

CONCLUSION

A Giant magnetostrictive material-fiber Bragg grating magnetic field sensors used in magnetic Bearings was investigated experimentally. Based on this study, the following conclusions can be drawn:

1. A novel FBG-GMM sensor was proposed to measure magnetic flux density, especially in small gap.

2. The FBG-GMM magnetic field sensor's properties were tested on a U-shape electromagnet test setup, the measured data were consistent with the theoretical prediction and the sensor' linear range was from 0.2T to 0.6T.

3. The FBG-GMM magnetic field sensor was introduced to measure a radial magnetic bearing's air-gap flux density. Static flux density measurement was performed through two FBG-GMM sensors and one temperature compensation FBG, and the measured data were consistent with the sensor properties obtained from the U-shape electromagnet test, which validated the FBG-GMM magnetic field sensor's feasibility.

ACKNOWLEDGEMENTS

This work was supported by the National Science Foundation of China (Project No. 51105285).

REFERENCES

[1] J.L. Cruz, A. Diez, M.V. Andres, A. Segura, B. Ortega, L. Dong, Fiber Bragg gratings tuned and chirped using magnetic fields, Electron. Lett. 33 (1997) 235–236.

[2] K.S. Chiang, R. Kancheti, V. Rastogi, Temperature-compensated fiber-Bragggrating-based magnetostrictive sensor for dc and ac currents, Opt. Eng. 42(2003) 1906–1909.

[3] D. Satpathi, J.A. Moore, M.G. Ennis, Design of a Terfenol-D based fiber-optic current transducer, IEEE Sens. J. 5 (2005) 1057–1065.

[4] C. Ambrosino, S. Campopiano, A. Cutolo, A. Cusano, Sensitivity tuning in Terfenol-D based fiber Bragg grating magnetic sensors, IEEE Sens. J. 8 (2008)1519–1520.

[5] A.A. Moghadas, M. Shadaram, Fiber Bragg grating sensor for fault detection in radial and network transmission lines, Sensors 10 (2010) 9407–9423.